Global Seismic Nowcasting with Shannon Information Entropy

John B Rundle[1,2,3,4,5], Alexis Giguere[1], Donald L. Turcotte[3], James P. Crutchfield[1,2]

[1] Department of Physics
University of California, Davis, CA

[2] Santa Fe Institute
Santa Fe, NM

[3] Department of Earth and Planetary Science
University of California, Davis, CA

[4]Jet Propulsion Laboratory
Pasadena, CA

[5]Tohoku University
Sendai, Japan

Abstract

Seismic nowcasting uses counts of small earthquakes as proxy data to estimate the current dynamical state of an earthquake fault system. The result is an Earthquake Potential Score (EPS) that characterizes the current state of progress of a defined geographic region through its nominal earthquake "cycle". The count of small earthquakes since the last large earthquake is the natural time that has elapsed since the large earthquake (Varotsos et al., 2006). In addition to natural time, there are other ways to characterize small earthquakes that include other types of data. One of these is Shannon Information Entropy ("information"), an idea that was pioneered by Shannon (1948). As a first step to adding seismic information into the nowcasting method, we develop a method for incorporating magnitude information into the natural time counts by using event self-information. We find in this first application of seismic information entropy that the EPS values are similar to the values using only natural time.

Introduction

The determination of earthquake risk for geographic regions is an old problem that has been associated with the development of methods for forecasting and prediction (Holliday et al, 2016; Scholz, 2002; WGCEP[1]). In many ways, the problem of earthquake forecasting bears similarities to the problem of forecasting in weather and economic systems (Jolliffe and Stephenson, 2003; OECD[2]). In all these cases, probabilities of future activity are calculated using physical or statistical models, and then validated by backtesting and prospective testing.

An associated question is the degree to which past and present conditions convey information about future conditions. For the case of weather forecasting, the continual improvement of forecasting methods is evidence that there is considerable information contained in past data, and that the improvement of data acquisition via satellite observations maps into better probabilities of future activity (Marshall et al., 2006).

An important goal is therefore to quantify the amount of information that is contained in past activity. In order to address this question, we begin with the simpler idea of nowcasting, and apply ideas from the field of Shannon Information Entropy. Nowcasting is a simpler form of risk estimation than forecasting, and is therefore readily amenable to analysis of information content.

Nowcasting

Nowcasting refers to the use of proxy data to estimate the current dynamical state of a driven complex system such as earthquakes, neural networks, or the financial markets (Rundle et al., 2016; refs). In previous papers (Rundle et al., 2016, 2017, 2018), a method to nowcast earthquakes has been presented based on the natural time count of small earthquakes after the last large earthquake in a defined, seismically active geographic region.

The basic idea is that the recurring pattern, or cycle, of "large earthquake-quiescence-large earthquake" is characterized by an "earthquake clock" that in some way quantitatively describes the region (e.g., Rogerson, 2018; Hill and Prejean, 2007). Nowcasting is a method that can be used to statistically define the current state of this earthquake clock.

In the nowcasting method, a "large" geographic region is identified in which a "local" region of interest is embedded. The primary assumption in the method is that the frequency-magnitude statistics of the large region are the same as the those of the local region. From a practical standpoint, this implies that the Gutenberg-Richter b-value is assumed to be the same in both regions.

In addition to these points, there have been a series of papers discussing the idea of earthquake triggering. This is associated with the idea of "clock advance"

whereby a previous earthquake will advance the earthquake clock of the region of interest so that a large earthquake would occur sooner than it otherwise would (e.g., Gomberg et al., 1998; Savage and Marone, 2008; Rogerson, 2018). For these applications, it is important to understand the current state of the earthquake clock, since a clock advance early in the earthquake cycle may not be as significant as a clock advance late in the earthquake cycle. Nowcasting provides at least an approximate answer to the question of the current state of the earthquake clock.

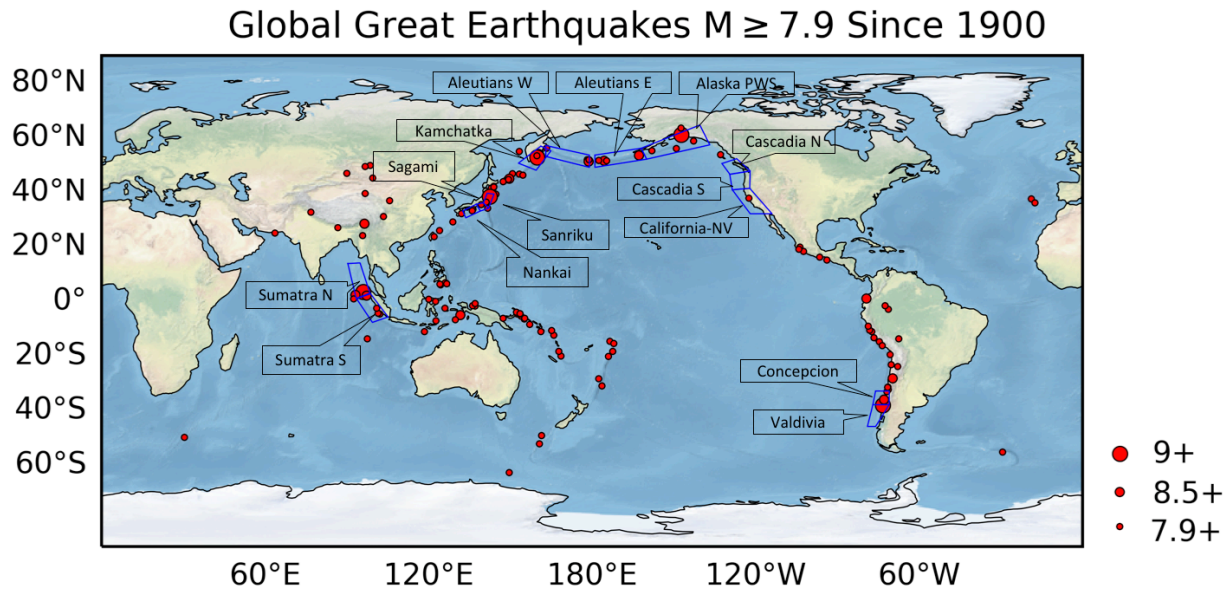

Data

The nowcasting technique relies on seismic catalogs that are complete, in the sense that all events whose magnitude is larger than a completeness threshold have been detected. In the large geographic region, many large earthquakes are required to define the inter-event statistics of the small earthquakes in natural time.

As an example, this paper considers the "large" geographic region to be the entire Earth, and the "small" regions to be polygonal source regions for great earthquakes. More specifically, we consider "large" earthquakes of magnitude $M \geq 7.9$, and "small" earthquakes of magnitude $6 \leq M < 7.9$. An example is shown in Figure 1, which displays all earthquakes of magnitude $M \geq 7.9$ occurring since 1900, together with 14 polygonal source regions. Note that while the exact choice of the source regions is arbitrary, they nevertheless encompass earthquake fault segments upon which historic earthquakes are known have occurred. These polygons were chosen

using methods analogous to those used to define seismic gap segments in previous studies (Kelleher et al., 1973; Nishenko, 1991; Scholz, 2002).

We then construct a histogram for the number of small earthquakes between the large earthquakes in the large geographic region. Focusing next on the small region, we count the number of small earthquakes that have occurred since the last large earthquake. Comparing this natural time count (Varotsos et al., 2006; Holliday et al, 2006) to the histogram in the large region determines the Earthquake Potential Score (EPS) from the Cumulative Distribution Function (CDF) constructed from the natural time histogram.

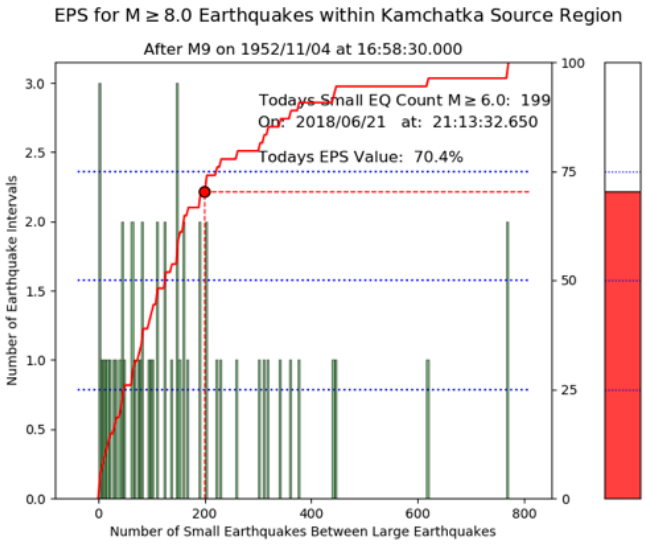

Figure 2. Current Earthquake Potential Score (EPS) for the Kamchatka source polygon. Vertical green bars are the histogram of counts of "small" earthquakes having $M \geq 6$ between the great earthquakes having $M \geq 8.0$. The red dot records the current count, 199, of small earthquakes in the polygon, with a corresponding EPS value of 70.4%.

An example of the EPS score is shown in Figure 2 for the Kamchatka source polygon. The M9.0 Kamchatka earthquake occurred in that polygonal source region on November 4, 1952 (ref). An associated tsunami generated by the earthquake led to the deaths of 10,000 to 15,000 persons in the Kuril islands (WSSPC[3]). Runups as high as 15 meters were observed locally, and runups as large as 1 meter were observed as far away as California.

The (green) vertical bars in Figure 1 represent the numbers of $6 \leq M < 7.9$ earthquakes between the $M \geq 7.9$ great earthquakes that occurred worldwide since 1950. The red curve ascending from lower left to upper right is the CDF corresponding to the histogram. The current count of 251 small earthquakes having magnitudes $6 \leq M < 7.9$ since the great earthquake in 1950 is indicated by the red dot in Figure 1, leading to an EPS value of 70.4%. The interpretation of this statistic is that the Kamchatka source polygon has achieved 70.4% of the progress of the typical earthquake cycle characterizing global great earthquakes, in terms of the number of small earthquakes intervening between the great earthquakes.

The current values of EPS scores for the other 13 source polygons is shown in Table 1. In some cases, the largest catalog earthquake that occurred in the source polygon is less than M7.9, and is indicated in the 4th column. In other columns...

Shannon Information Entropy

Shannon information entropy was developed as a means to characterize the information content transmitted between a source and a receiver by means of a communication channel (Shannon, 1948; Cover and Thomas, 1991; Stone, 2015). In his 1948 paper, Shannon described a method for computing a metric for the information delivered from a source to a receiver using only binary (yes/no) decisions. Given an "alphabet" of symbols, Shannon showed that the number of decisions needed to send a symbol from the source to the receiver defines the information content ref of the communication. He related this to the degree of surprise, or "surprisal", of unanticipated content embedded in the signal.

The typical example is "Alice" sending a word to "Bob" by means of a binary digital communication device. Alice must send the message letter-by-letter. So the question is, how many binary digits must Alice send to convey a single letter? If each letter in the alphabet is equally probable (it is not!), the answer is 4.7 bits of information. This value can be determined by the use of equation (1) below, using a letter probability $p_i = \frac{1}{26}$.

The principal objective of the present paper is to examine the role of Shannon information entropy, and similar arguments, in earthquake physics, and by extension, in other driven threshold systems. We take a somewhat different approach than (Giguere et al., 2018) who used information theory to derive a new magnitude-frequency relation for earthquake magnitudes. Here we use the known earthquake frequency-magnitude statistics to confront the issue of how to measure the amount of information that an earthquake occurrence is delivering to an observer. This problem may have significance to the problem of earthquake forecasting and nowcasting ref.

A reason to believe that information might be contained in earthquake sequences is the idea that neural networks and earthquakes bear strong similarities in terms of the governing equations (Rundle et al., 2002; Hopfield, 1994; Hertz and Hopfield, 1995). It is known that neural networks convey information, and that Shannon information entropy methods are used to characterize their information content (Marzen et al., 2015; Marzen and Crutchfield, 2017).

In these neural network systems, it is known that neurons are simple elements that emit action potentials or voltage "spikes" in response to driving currents (Hopfield, 1994). Once a neuron fires, typically at a level of -53 mV, the voltage resets to around -70 mV, followed by a refractory period during which the neuron does not fire. It is believed that the information is contained in the temporal spacing between the spikes.

On the other hand, earthquakes are caused by tectonic driving forces that lead to a sudden slip event associated with a sudden change in fault stress or stress "spike". While neural networks are an electrical system, earthquakes are a

mechanical system. The common features of these two systems have been listed by (Hopfield, Hertz and Hopfield, and Rundle et al). For these reasons, we pursue a program similar to the (Marzen et al., 2015; Marzen and Crutchfield, 2017) approach to analyze the information content of earthquake sequences. We begin with an analysis of the information contained by the magnitude of the events in earthquake sample sequences.

To understand information entropy, one starts with an "alphabet" of symbols, each symbol indexed by the integer i. In our case, the alphabet will be a sequence of discrete magnitude "bins" centered on a value m_i, each bin being of width $\Delta m \rightarrow 0$. Although we will use earthquake magnitude, some studies suggest that additional information might be found by evaluating the probabilities of earthquake intervals. The probability that an earthquake has a magnitude m_i is denoted as p_i.

For a system having discrete states indexed by an integer i, Shannon defined the self-information I_i as:

$$I_i = -\log_2(p_i) \tag{1}$$

(Cover and Thomas, 1991; Stone, 2015).

The equation for average or expectation of Shannon self-information is:

$$I \equiv < I_i > = \sum_i p_i \log_2(p_i) \tag{2}$$

Note that it is required that $0 \leq p_i \leq 1$ and that $\sum_i p_i = 1$. As a result, $I \geq 0$. Also, note that by construction, I is an expectation or average. As a common practice, we will refer to I as simply the Shannon information.

Although we will use earthquake magnitude, the neural network studies suggest that additional information might be found by evaluating the probabilities of earthquake intervals. In this respect, we might find ourselves discussing the similarities and distinctions between magnitude entropy and interval entropy. Similarly, we might find ways to evaluate entropy of slip-rate distributions, and other earthquake related quantities. A potentially important question might be, is entropy change in one variable correlated with entropy change in another variable? This might imply some sort of information principle important to earthquake predictability.

Magnitude Information

We first examine magnitude information, and to do so, we start with the Gutenberg-Richter distribution:

$$N(\geq m) = 10^{a-bm} \tag{3}$$

Equation (5) can be interpreted as the survivor distribution:

$$Q(m\,|m_c)\ \equiv\ N(\geq m) \tag{4}$$

for magnitudes m, given the catalog completeness magnitude m_c. The associated cumulative distribution function P(m | m_c) is then:

$$P(m|m_c) = 10^{a-bm} \tag{5}$$

Using the substitution $\beta \equiv b\ln(10)$, the associated probability density function $\rho(m)$ in magnitude space is then found from differentiating (5):

$$\rho(m) = \beta e^{\beta(m_c-m)} \tag{6}$$

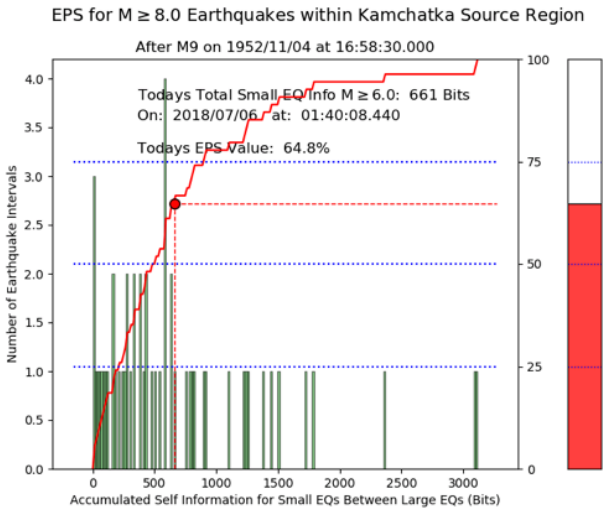

Figure 3. Current Earthquake Potential Score (EPS) for the Kamchatka source polygon. Vertical green bars are the histogram of self-information in bits for "small" earthquakes having M≥6 between the great earthquakes having M≥8.0. The red dot records the current self-information value, 661 bits, of small earthquakes in the polygon, with a corresponding EPS value of 64.8%.

We note that the for the discrete case, the probability p(m_Δ) that the magnitude lies between (m, m + Δm) is:

$$p(m_\Delta) = P(m \leq m_\Delta \leq m + \Delta m) = 10^{b(m_c - m)}(1 - 10^{-b\Delta m}) \tag{7}$$

where Δm is the coarse-grained magnitude element.

In this case, the "alphabet" of symbols being transmitted is the sequence of magnitude bins beginning at the completeness magnitude m_c, and having width Δm. For this numerical calculation, the probability for a bin centered on magnitude value m can be obtained from equation (6):

$$p(m_\Delta) = \varrho(m_\Delta)\Delta m\ =\ \beta e^{(m_c-m)}\,\Delta m \tag{8}$$

Results

Following on the approach of Giguere et al. (2018) and Rundle et al. (2018), we wish to extend the natural time count in the nowcasting technique to a statistic that includes not only the natural time count, but also the earthquake magnitude. In future work, we also want to account for the time intervals between small earthquakes, but for the present, we focus on magnitude. Results are shown in Figure 2.

Table 1: Natural Time Nowcast

Location (Source Polygon)	EPS(%) Score on 2018/06/27 at 14:58:30 PT	Date Most Recent Large EQ in Polygon	Mag Most Recent Large EQ in Polygon	Nat. Time Count on 2018/06/27 at 14:58:30 PT	Current Potential Magnitude
AleutionsE	77.8	1946/04/01	8.6	251	8.2
Kamchatka	70.4	1952/11/04	9	199	8.2
CascadiaS	69.4	1922/01/31	7.3	26	7.3
CascadiaN	55.3	1946/06/23	7.5	28	7.4
California-Nevada	43.0	1906/04/18	7.9	69	7.7
AleutionsW	40.7	1965/02/04	8.7	100	7.9
AlaskaPWS	38.9	1964/03/28	9.2	88	7.8
Sagami	25.9	1923/09/01	8.1	64	7.7
SumatraN	25.9	2004/12/26	9.1	62	7.7
Sanriku	25.9	2011/03/11	9.1	58	7.7
SumatraS	25.9	2005/03/28	8.6	56	7.6
Valdivia	20.4	1960/05/22	9.5	46	7.6
Concepcion	18.5	2010/02/27	8.8	40	7.5
Nankai	13.0	1946/12/20	8.3	22	7.3

We replace the counts of small earthquakes with the sum of the self information in magnitude space using equations (1) and (8) (see Giguere et al., 2018; Rundle et al., 2018). Further, we assume that the coarse-grained magnitude element is given by the typical magnitude resolution of $\Delta m \approx 0.1$. The result is shown in Figure 3 for the same polygon as in Figure 2, the Kamchatka source polygon, source of the 1952 M9.0 Kamchatka earthquake and tsunami. Here the EPS is 64.8%, compared to the previous natural time count-based value of 70.4%.

Table 2: Natural Time - Information Nowcast

Location (Source Polygon)	EPS(%) Score on 2018/07/10 at 10:05:19 PT	Date Most Recent Large EQ in Polygon	Mag Most Recent Large EQ in Polygon	Nat. Time Count on 2018/07/10 at 10:05:19 PT	Current Potential Magnitude
AleutionsE	74.1	1946/04/01	8.6	841	8.2
CascadiaS	66.7	1922/01/31	7.3	95	7.3
Kamchatka	64.8	1952/11/04	9	661	8.2
CascadiaN	47.9	1946/06/23	7.5	88	7.4
California-Nevada	44.3	1906/04/18	7.9	266	7.7
AleutionsW	38.9	1965/02/04	8.7	354	7.9
AlaskaPWS	35.2	1964/03/28	9.2	317	7.8
Sagami	24.1	1923/09/01	8.1	216	7.7
SumatraS	24.1	2005/03/28	8.6	218	7.6
SumatraN	24.1	2004/12/26	9.1	208	7.7
Sanriku	22.2	2011/03/11	9.1	185	7.7
Valdivia	18.5	1960/05/22	9.5	159	7.6
Concepcion	18.5	2010/02/27	8.8	127	7.5
Nankai	13.0	1946/12/20	8.3	84	7.3

Comparing Figures 2 and 3, it can be seen that there is relatively little difference between the values for the EPS. Data for the remainder of the 13 source polygons is shown in Table 2, analogous to Table 1. As is discussed more extensively in Giguere et al. (2018), most of the information is contained in the smaller events, primarily because there are so many more of them. This raises the question of whether this method could be modified to more strongly emphasize the larger of the small events.

To emphasize this last point, we show in Figure 4 the frequency-magnitude relation for a region of radius 1000 km around Tokyo, Japan. In Figure 4a, data are for the time interval from 1/1/1970 through the last event prior to the M9.1 earthquake on March 11, 2011. Figure 4b shows the data following the M7.7 aftershock up to the present.

Figure 4a shows that the data are well fit at almost all magnitude intervals by a

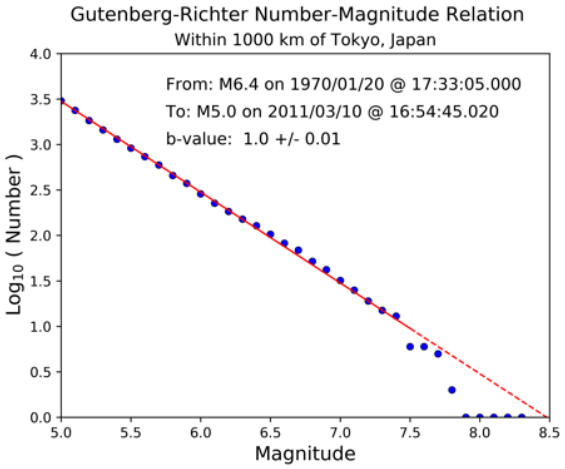

Figure 4(a). Magnitude-frequency data for the spatial region within 1000 km of Tokyo, Japan, prior to the M9.1 mainshock on March 11, 2011. Solid red line indicates the magnitude range fit by the scaling line, from M5.0 to M7.5.

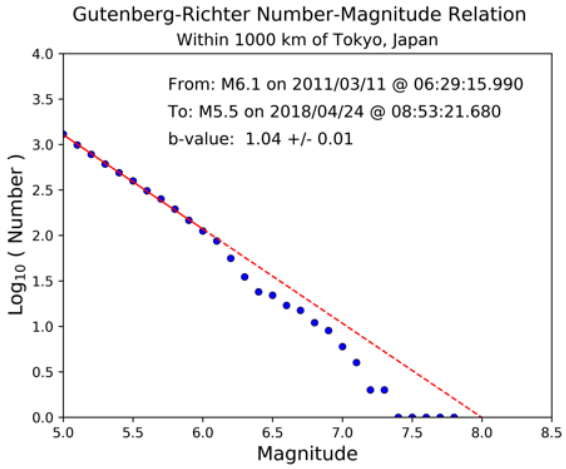

Figure 4(b). Magnitude-frequency data for the spatial region within 1000 km of Tokyo, Japan, following the M7.7 aftershock on March 11, 2011. Solid red line indicates the magnitude range fit by the scaling line, from M5.0 to M6.0.

Gutenberg-Richter scaling line having a slope, or b-value of 1.0 ± 0.1. This can be considered to be the long-term average behavior of earthquakes in the region. On the other hand, the data in Figure 4b show that the scaling line is first re-established at the small magnitude end, and that there is a deficiency of larger magnitude earthquakes relative to the scaling line. The b-value of the scaling line is 1.04 ± 0.1, nearly the same as in Figure 4a. This deficit in larger earthquakes is eventually removed as larger earthquakes occur.

Summary and Conclusions

This paper has been concerned with a first study to incorporate measures of Shannon information entropy into the nowcasting method. A question that has been addressed elsewhere is the issue of the sensitivity of the EPS values to the data used to define the histogram and therefore the CDF. We have shown in companion papers (Rundle et al., 2017; Rundle et al., 2018) that the nowcasting method is generally not very sensitive to the choice of large spatial region defining the histogram, leading to a standard error of approximately $\pm 10\%$. However, the method is strongly sensitive to issues of catalog completeness (Rundle et al., 2018).

We have found that in this first study, the results of using magnitude information

are similar to those found using only natural time counts of events. The primary reason for this is that even though large magnitude events carry more information than small magnitude events, there are many more small magnitude events at approximately the catalog completeness magnitude. Thus the information entropy at these small events dominates the total self-information sum. Further work will investigate techniques to focus attention on primarily the largest events. In future work we also plan to incorporate temporal information in the Shannon information measures through the use of methods similar to those developed in connection with models for Epidemic Type Aftershock Sequences and their derivative methods (Ogata, 2004; Helmstetter and Sornette, 2003; Turcotte et al., 2007).

Acknowledgements

The research of JBR was supported in part by NASA grant (NNX17AI32G) to UC Davis (nowcasting) and in part by DOE grant (DOE DE-SC0017324) to UC Davis (information entropy). The research of AG was supported by DOE grant (DOE DE-SC0017324) to UC Davis.

Notes

[1] http://www.wgcep.org/overview
[2] http://www.oecd.org/economy/oecd-forecasts-during-and-after-the-financial-crisis-a-post-mortem.htm
[3] www.wsspc.org/resources-reports/tsunami-center/significant-tsunami-events/1952-kamchatka-tsunami/

References

Cover, TM and JA Thomas, *Elements of Information Theory*, John Wiley, NY, (1991) ISBN 0-471-06259-6

Giguere, A, JB Rundle and M Yoder, Shannon Information Theory: Applications to Earthquakes and Driven Threshold Systems, Submitted to *J. Stat. Phys* (2018)

Gomberg, J, Beeler, NM, Blanpied, M, and Bodin, P, Earthquake triggering by transient and static deformations, *J. Geophys. Res*., 103, 24,411-24,426 (1998).

Helmstetter, A., and D. Sornette, D, Predictability in the Epidemic-Type Aftershock Sequence model of interacting triggered seismicity, *J. Geophys. Res*., 108(B10), 2482, (2003) doi:10.1029/2003JB002485.

Hertz, AVM and Hopfield, JJ, Phys. Rev. Lett. 75, 1222-1225 (1995) doi.org/10.1103/PhysRevLett.75.1222

Hill DP and Prejean SG, Dynamic triggering, in Earthquake seismology, vol. 4, G. Schubert, H. Kanamori, Eds. *Treatise on Geophysics*, Schubert, G (Editor-in Chief) (Elsevier, Amsterdam), pp. 257–291 (2007)

Holliday, JR, Graves, WR, Rundle, JB, and Turcotte, DL, Computing earthquake probabilities on global scales, *Pure. Appl. Geophys*., 173, 739-748 (2016). DOI 10.1007/s00024-014-0951-3

Hopfield, JJ, Neurons, Dynamics and Computation, *Phys. Today*, 47, 40-46 (1994) https://doi.org/10.1063/1.881412

Kelleher, J. A., L. R. Sykes, and J. Oliver, Possible criteria for predicting earthquake locations and their applications to major plate boundaries of the Pacific and Caribbean, *J. Geophys. Res*., 78, 2547–2585 (1973)

Marshall, JL et al., Improving global forecasting and analysis with AIRS, *Bull. Amer. Met. Soc*., 87, 891-894 (2006)

Main, IG, and Al-Kindy, FH, . Entropy, energy, and proximity to criticality in global earthquake populations. *Geophys. Res. Lett*., 29(7) (2002)

Marzen, SE and JP Crutchfield, Structure and randomness of continuous-time, discrete-event processes, *J Stat Phys* (2017) 169:303–315 DOI 10.1007/s10955-017-1859-y

Marzen, SE, DeWeese, MR, and Crutchfield, JP, Time resolution dependence of information measures for spiking neurons: Atoms, scaling, and universality, *Santa Fe Institute Working Paper*. arXiv:1504.04756v1[q-bio.NC] 18 April (2015)

Nicholas V. Sarlis, Efthimios S. Skordas, Panayiotis A. Varotsos, Alejandro Ramírez-Rojas, E. Leticia Flores-Márquez, Natural time analysis: On the deadly Mexico M8.2 earthquake on 7 September 2017, *Physica A* 506 (2018) 625–634.

Nishenko, S. P., Circum-Pacific seismic potential—1989–1999, *Pure Appl. Geophys.*,135, 169–259 (1991)

NV Sarlis, ES Skordas, and PA Varotsos. The change of the entropy in natural time under time-reversal in the olami–feder–christensen earthquake model. *Tectonophysics,* 513(1):49–53, 2011.

Ogata, Y., Space-time model for regional seismicity and detection of crustal stress changes, *J. Geophys. Res*., 109, B03308, (2004) doi:10.1029/2003JB002621.

PA Varotsos, NV Sarlis, ES Skordas, HK Tanaka, and MS Lazaridou. Attempt to distinguish long-range temporal correlations from the statistics of the increments by natural time analysis. *Phys. Rev. E*, 74(2):021123, 2006.

Panayiotis A Varotsos, Nicholas V Sarlis, Efthimios S Skordas, and Haruo Tanaka: A plausible explanation of the b-value in the gutenberg-richter law from first principles. *Proc. of the Japan Acad*., Series B, 80(9):429–434, 2004.

Rogerson, PA, Statistical evidence for long-range space-time relationships between large earthquakes, *J. Seismology*, published online, July 30, 2018: doi.org/10.1007/s10950-018-9775-4

Rundle, JB, Tiampo, KF, Klein, W and Martins, JSS, Self-organization in leaky threshold systems: The influence of near mean field dynamics and its implications for earthquakes, neurobiology and forecasting, *Proc. Nat. Acad. Sci. USA*, 99, Supplement 1, 2514-2521, (2002)

Rundle, JB, Luginbuhl, M, Khapikova, P, Turcotte, DL, Donnellan, A and McKim, G, Nowcasting global earthquakes and tsunami sources, submitted to *Pure Appl. Geophys*, (2018).

Savage, HM, and Marone, C, Potential for earthquake triggering from transient deformations, J. Geophys. Res., 113, B05302 (2008)doi:10.1029/2007JB005277

Scholz, C. H., *The Mechanics of Earthquakes and Faulting*, , 2nd ed., 471 pp., Cambridge Univ. Press, New York (2002)

Shannon, C.E., "A Mathematical Theory of Communication", *Bell System Technical Journal*, 27, pp. 379–423 & 623–656, July & October (1948).

Stone, JV, *Information Theory, A Tutorial Introduction*, Sebtel Press, (2015) ISBN978-0-9563728-5-7

Telesca, L, Lovallo, M, El-Ela Amin Mohamed, A, ElGabry, M, El-Hady, S, Abou Elenean, KM, and ElShafey Fat ElBary, R, Informational analysis of seismic sequences by applying the Fisher information measure and the Shannon entropy: An application to the 2004–2010 seismicity of Aswan area (Egypt), *Physica A*: *Stat. Mech. Appl.*, 391(9):2889–2897 (2012).

Turcotte, DL, Holliday, JR, and Rundle, J, BASS, an alternative to ETAS, *Geophys. Res. Lett.,* 34, L12303, doi:10.1029/2007GL029696 (2007)

Vallianatos, F, Michas, G, Papadakis, G, and Sammonds, P, A nonextensive statistical physics view to the spatiotemporal properties of the June 1995, Aegean earthquake (M6. 2) aftershock sequence (West Corinth rift, Greece), *Acta GeoPhysica*, 60(3):758–768 (2012).

Varotsos,PA, Sarlis, NV, Skordas, ES, Tanaka, HK and Lazaridou, MS, Attempt to distinguish long-range temporal correlations from the statistics of the increments by natural time analysis, *Phys. Rev. E*, 74, 021123 (2006).